Histological And Radiographical Evaluation Of Maxillary Sinus Floor Augmentation Using Osteoplant Flex Sheets

Thesis

Submitted to the Faculty of Dentistry, Ain Shams University in partial fulfillment of the requirements of Doctorate degree in Oral and Maxillofacial Surgery

By

Karim Mohamed Mahmoud Abdel Mohsen

B.D.S Ain Shams University (2001)

M.D.S Ain Shams University (2008)

Oral and Maxillofacial Surgery Department
Faculty of Dentistry
Ain Shams University
(2012)

Histological And Radiographical Evaluation Of Maxillary Sinus Floor Augmentation Using Osteoplant Flex Sheets

Thesis

Submitted to the Faculty of Dentistry, Ain Shams University in partial fulfillment of the requirements of Doctorate degree in Oral and Maxillofacial Surgery

Supervisors

Ahmed Barakat

Professor of
Oral and Maxillofacial Surgery
Faculty of Oral and Dental Medicine
Cairo University

Mohamed Katamish

Assistant Professor of Oral and Maxillofacial Surgery Faculty of Dentistry Ain Shams University

Khaled AbdelMoneam

Lecturer of Oral and Maxillofacial Surgery
Faculty of Dentistry
Ain Shams University

Oral and Maxillofacial Surgery Department
Faculty of Dentistry
Ain Shams University
(2012)

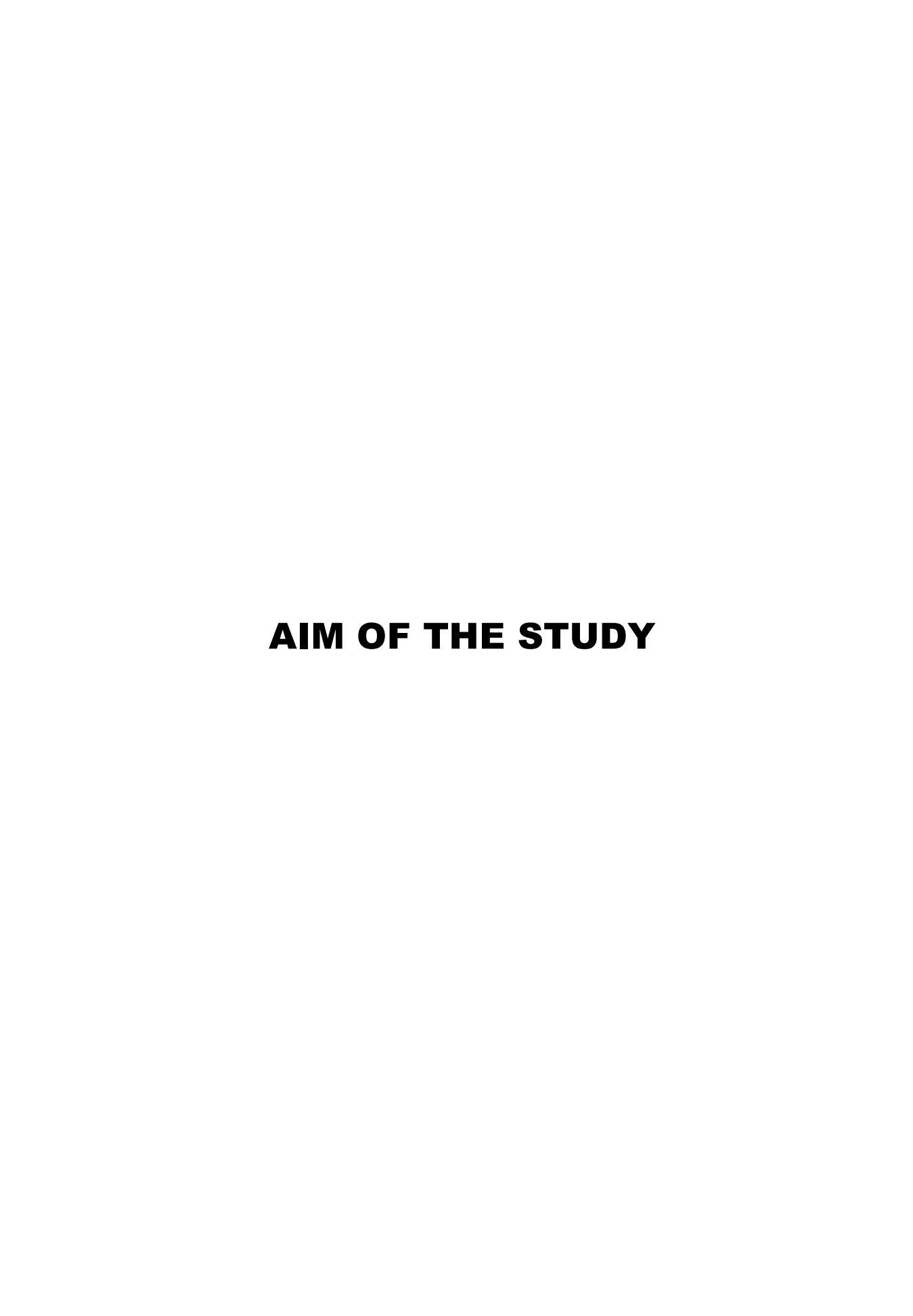
ACKNOWLEDGMENT

My special thanks and deep obligations to *Dr / Iman Helmy*, Professor of Oral Pathology, Faculty of Dentistry, Ain Shams University for her great efforts, considerable assistance and for dedicating much of her precious time to accomplish this work.

I also like to thank sincerely *Dr / Hani El Zoheiry*, Assistant Lecturer of Oral Radiology, Faculty of Dentistry, Ain Shams University for his unique effort, precious time, and valuable guidance during this work.

I would also like to express my gratitude to all my colleagues in the Oral and Maxillofacial Surgery Department, Faculty of Dentistry, Ain Shams University, for their valuable support throughout the performance of this work.

Last but not least I would like to thank my family for their great support and valuable advice during this work.



This study will be conducted to evaluate clinically, radiographically and histologically the quality of the formed bone in maxillary sinus lifting procedures using Osteoplant Flex as a bone substitute.

LIST OF CONTENTS

Title	Page Number
Introduction	1
Review of literature	4
Aim of the study	37
Materials and methods	39
Results	62
Discussion	76
Summary and conclusions	86
References	89
Arabic summary	116

LIST OF FIGURES

Figure No.	Title	Page No.
Figure 1:	Photograph showing horizontal crestal incision a releasing incision down to the depth of the vestibular	
Figure 2:	Photograph showing mucoperiosteal flap reflected to the level of the malar buttress	- •
Figure 3:	Photograph showing an oval osteotomy in the latthe maxillary sinus made by a no.8 round diamond	
Figure 4:	Photograph showing gentle insertion of a elevator/curette along the margin of the crewindow.	eated access
Figure 5:	Photograph showing the space created between antral floor and the elevated maxillary sinus mem	•
Figure 6:	Photograph showing an easily adaptable hydr Osteoplant Flex sheet that has reached the plastic	
Figure 7:	Photograph showing insertion of the first Osteoplant Flex sheet into the sinus cavity to sinus membrane in the desired elevated position.	maintain the
Figure 8:	Photograph showing insertion of the cut small posteoplant Flex sheet to fill the space between the floor and the Osteoplant Flex sheet	e bony antral

Figure No.	Title Pag	ge No.
Figure 9:	Photograph showing a resorbable biocollagen me barrier modeled and adapted to the access window ar by titanium tacs	nd fixed
Figure 10:	Photograph showing surgical guide for implant insertion	on 54
Figure 11:	Photograph showing crestal incision performed for insertion	•
Figure 12:	Photograph showing mucoperiosteal flap reflected su to expose the edentulous bony ridge	-
Figure 13:	Photograph showing trephine drill obtaining the bowith the surgical guide secured in place	
Figure 14:	Photograph showing bone core released from the drill and fixed in 10% neutral buffered formalin solution	•
Figure 15:	Photograph showing the dental implants inserted in place covered by their healing screws	
Figure 16:	Radiograph of an axial slice showing the sagittate passing through the mesial tooth and along the ridge between the buccal and lingual cortices.	midway

Figure No.	Title Page No.	•
Figure 17:	Radiograph of a sagittal slice showing the coronal plan passing at the point showing maximum maxillary sinu pneumatization and lying parallel to a line drawn along the long axis of the mesial tooth and passing through its root aperates the same statement of the same showing the coronal plan passing at the point showing maximum maxillary sinu pneumatization and lying parallel to a line drawn along the long axis of the mesial tooth and passing through its root aperates.	is ie x
Figure 18:	Radiograph of a coronal slice showing measurement of the preoperative bone height from the crest of the ridge to the maxillary sinus floor parallel to the sagittal plane 58	ie
Figure 19:	Radiograph of a coronal slice showing measurement of the postoperative bone height from the crest of the ridge to the maxillary sinus floor parallel to the sagittal plane	ie
Figure 20:	Radiograph of a coronal slice showing two rectangles with the same dimensions measuring the average radiographic bondensity within the region of interest, one lying completely within the new regenerated bone, and the other lying completely within the old original bone	y g
Figure 21:	Photomicrograph after correction of brightness and contrast	
Figure 22:	Photomicrograph converted to gray scale 69	0
Figure 23:	Photomicrograph showing thresholded bone	1

Figure No.	Title	Page No.
Figure 24:	Radiograph of a sagittal slice showing the new bone, the original old bone and the interface clear between them	rly delineated
Figure 25:	Bar chart representing comparison between properative bone height measurements	_
Figure 26:	Bar chart representing comparison between properative radiographic bone density measurement	•
Figure 27:	Photomicrograph showing multiple new bone different sizes with fibrovascular tissue	
Figure 28:	Photomicrograph showing multiple newly for trabeculae anastomozing with each other	
Figure 29:	Photomicrograph showing new bone formation the old bone	
Figure 30:	Bar chart showing comparison between total bon new and old bone	
Figure 31:	Bar chart showing comparison between trabecular and old bone	
Figure 32:	Bar chart showing comparison between trabecular new and old bone	

Figure No.	Title	Page No.
Figure 33:	Bar chart showing comparison between area	fractions of new
	and old bone	75

LIST OF TABLES

Table No.	Title	Page No.
Table (I):	Descriptive statistics for the values of bone radiographic bone density of both the newly regent and the original old bone	nerated bone
Table (II):	Results of Wilcoxon signed-rank test for the between mean bone height measurements pre-operatively	- and post-
Table (III)	Results of Wilcoxon signed-rank test for the between mean radiographic bone density pre-operatively	and post-
Table (IV):	Descriptive statistics for the difference in histological measurements between the newly bone and the original old bone	regenerated
Table (V):	Results of Wilcoxon signed-rank test for the between mean total bone areas of the newly reger and original old bone	nerated bone
Table (VI):	Results of Wilcoxon signed-rank test for the between mean trabecular sizes of the newly regent and original old bone	nerated bone

LIST OF TABLES (Cont...)

Table No.	Title	Page No.
Table (VII):	Results of Wilcoxon signed-rank test for the	comparison
	between mean tracecular counts of the newly	regenerated
	bone and original old bone	74
	D. I. C.W.	
Table (VIII):	Results of Wilcoxon signed-rank test for the	comparison
	between mean area fractions of the newly regen	erated bone
	and original old bone	75

LIST OF ABBREVIATIONS

MSE Membrane Sinus Elevator technique

TCP Tricalcium Phosphate

HA Hydroxyapatite

BG Bioactive Glass

BMP Bone Morphogenic Proteins

PMCB Particulate Marrow and Cancellous Bone

FDBA Freeze-Dried Bone Allograft

DFDBA Demineralized Freeze Dried Bone Allograft

DBM Demineralized Bone Matrix

PRP Platelet-Rich Plasma

PDGF Platelet-Derived Growth Factor

TGF-β Transforming Growth Factor

ABC Autogenous Bone-derived Cells

CT Computerized Tomogram

CBCT Cone Beam Computerized Tomogram

QCT Quantitative Computerized Tomogram

QCBCT Quantitative Cone Beam Computerized Tomogram

MDCT Multi Detector Computerized Tomogram

ESS Endoscopic Sinus Surgery

ROI Region Of Interest

FOV Field Of View

H & E Hematoxylin and Eosin

SD Standard Deviation

HU Hounsfield Units